

OPEN

# Comparison of composite and segmental methods for acquiring optical axial length with swept-source optical coherence tomography

So Goto<sup>1,2,3</sup>, Naoyuki Maeda<sup>1\*</sup>, Toru Noda<sup>2</sup>, Kazuhiko Ohnuma<sup>4</sup>, Shizuka Koh<sup>1</sup>, Ikko Iehisa<sup>2</sup> & Kohji Nishida<sup>1,5</sup>

This study compared the optical axial length (AL) obtained by composite and segmental methods using swept-source optical coherence tomography (SS-OCT) devices, and demonstrated its effects on the post-operative refractive errors (RE) one month after cataract surgery. Conventional AL measured with the composite method used the mean refractive index. The segmented-AL method used individual refractive indices for each ocular medium. The composite AL ( $24.52 \pm 2.03$  mm) was significantly longer ( $P < 0.001$ ) than the segmented AL ( $24.49 \pm 1.97$  mm) among a total of 374 eyes of 374 patients. Bland–Altman analysis revealed a negative proportional bias for the differences between composite and segmented ALs. Although there was no significant difference in the RE obtained by the composite and segmental methods ( $0.42 \pm 0.38$  D vs  $0.41 \pm 0.36$  D, respectively,  $P = 0.35$ ), subgroup analysis of extremely long eyes implanted with a low power intraocular lens indicated that predicted RE was significantly smaller with the segmental method ( $0.45 \pm 0.86$  D) than that with the composite method ( $0.80 \pm 0.86$  D,  $P < 0.001$ ). Segmented AL with SS-OCT is more accurate than composite AL in eyes with extremely long AL and can improve post-operative hyperopic shifts in such eyes.

The accurate calculation of intraocular lens (IOL) power is crucial for achieving desirable refractive outcomes after cataract surgery. Post-operative refractive errors are mainly dependent on the following four factors: corneal power, axial length (AL), post-operative IOL position, and IOL quality (i.e. the error from variability in IOL power). Earlier studies have shown that 17–36% of post-operative refractive errors arise from imprecise AL measurements<sup>1,2</sup>. Historically, ultrasound biometry has been the most commonly used technique for measuring AL, anterior chamber depth (ACD), and crystalline lens thickness<sup>3</sup>. The immersion technique is generally considered to be more accurate than the contact technique in ultrasound biometry. However, the development of partial coherence interferometry (PCI) has led to more advanced optical biometry systems, which are ten times more precise than ultrasound for measuring AL<sup>4</sup>. PCI-based systems are now widely used and recognised as the gold standard for measuring ocular biometric parameters<sup>4–7</sup>.

It should be noted that optical and acoustic ALs are not equivalent, because the retinal pigment epithelium (RPE) is the endpoint of the optical measurements, and the internal limiting membrane (ILM) is the endpoint of the ultrasonic measurements. Moreover, the segmental method for AL determination includes the individual sound velocity of each component and the composite method uses the average sound velocity for all the components. Both methods are available for measuring the AL using ultrasound. On the other hand, the composite method measures AL optically via the mean group refractive index for all the components. Recently, segmented ALs measured by an optical low-coherence reflectometry (OLCR) biometer with a peak wavelength of 820 nm

<sup>1</sup>Department of Ophthalmology, Osaka University Graduate School of Medicine, Osaka, Japan. <sup>2</sup>Department of Ophthalmology, National Hospital Organization, Tokyo Medical Center, Tokyo, Japan. <sup>3</sup>School of Optometry and Vision Science, University of California Berkeley, California, 94720, USA. <sup>4</sup>Laboratorio de Lente Verde, Chiba, Japan. <sup>5</sup>Integrated Frontier Research for Medical Science Division, Institute for Open and Transdisciplinary Research Initiatives (OTRI), Osaka University, Osaka, Japan. \*email: [nmaeda@ophthal.med.osaka-u.ac.jp](mailto:nmaeda@ophthal.med.osaka-u.ac.jp)

	SS-OCT-based biometer			AS-OCT					
	Mean	Min	Max	Mean	Min	Max	Difference	R	P
Corneal thickness (um)	530 ± 31	418	611	544 ± 30	467	625	-13.6 ± 9.06	0.96	<0.001
Anterior chamber depth (mm)	3.15 ± 0.40	2.16	4.23	3.25 ± 0.42	1.96	4.25	-0.10 ± 0.12	0.96	<0.001
Aqueous depth (mm)	2.62 ± 0.40	1.62	3.71	2.70 ± 0.42	1.35	3.71	-0.08 ± 0.12	0.96	<0.001
Lens thickness (mm)	4.63 ± 0.40	3.33	5.79	4.65 ± 0.39	3.4	5.83	-0.02 ± 0.12	0.96	<0.001
Vitreous length (mm)	16.74 ± 1.91	13.44	24.78	16.89 ± 1.83	13.69	24.60	-0.15 ± 0.12	1.00	<0.001

**Table 1.** Comparison of optical biometry measurements acquired with a swept-source optical coherence tomography-based biometer and swept-source anterior segment optical coherence tomography ( $n = 374$  eyes). Data are presented as the mean standard deviation as applicable. SS-OCT = swept-source optical coherence tomography, AS-OCT = anterior segment optical coherence tomography, Min = minimum, Max = maximum, R = correlation coefficient.

were reported to be longer in short eyes and shorter in long eyes, compared to those obtained by composite ALs<sup>8,9</sup>. Although OLCR and PCI can measure the AL with greater precision than ultrasound and do not require any contact with the eye, the mis-segmentation of cornea or crystalline lens is difficult to detect, because OLCR and PCI provide axial and intraocular distances on an A-scan information without two-dimensional cross-sections of the images.

A second generation anterior segment swept-source optical coherence tomography (AS-OCT) was recently developed<sup>10–12</sup>. This novel, but commercially-available, AS-OCT system has an improved scan rate, depth capacity, and density assessment, allowing for sharper images of the anterior and posterior surfaces of the cornea, crystalline lens, and IOL. As a result, corneal thickness, ACD, aqueous depth (AQD: the distance between the corneal endothelium and the lens surface), and lens thickness can be automatically measured using AS-OCT with good repeatability and reproducibility<sup>10–12</sup>. Moreover, a newly introduced optical biometer that is also based on swept-source optical coherence tomography (SS-OCT) has been shown to generate repeatable and reproducible measurements<sup>13–16</sup>.

The current study compared optical ALs obtained with the conventional composite method and the segmental method using SS-OCT based devices and examined the differences in post-operative refractive errors following cataract surgery.

## Results

A total of 374 eyes of 374 patients (251 women [67.1%]) were included in this study. Patients had a mean age of  $76.1 \pm 8.3$  years (range: 40–96 years). All eyes had successful phacoemulsification with IOL implantation. AcrySof Toric and AN6MA IOLs were implanted in 358 and 16 eyes, respectively.

Table 1 summarises the ocular dimensions including the corneal thickness, ACD, AQD, lens thickness, and vitreous length measured with SS-OCT and AS-OCT. These values were significantly different when measured with the two instruments ( $P < 0.001$ ). The intraclass correlation coefficient was 0.992 for the corneal thickness, 0.999 for AQD, and 0.998 for the lens thickness, indicating good agreement for these parameters.

The mean composite  $AL_{RPE}$  was  $24.81 \pm 1.94$  mm (range: 21.52 to 32.93 mm) and the mean segmented  $AL_{RPE}$  was  $24.79 \pm 1.97$  mm (range: 21.42 to 32.99 mm). These values were significantly different ( $P < 0.001$ ), but there was a significant correlation between the two values ( $R = 1.00$ ). The mean composite  $AL_{ILM}$  was  $24.52 \pm 2.03$  mm (range: 21.09 to 33.01 mm) and the mean segmented  $AL_{ILM}$  was  $24.49 \pm 1.97$  mm (range: 21.12 to 32.69 mm). These values were also significantly correlated ( $R = 1.00$ ,  $P < 0.001$ ). The mean difference between the composite and segmented  $AL_{ILM}$  was  $0.038 \pm 0.067$  mm.

The Bland–Altman analysis revealed a negative proportional bias between the segmented and composite AL, indicating that the difference between segmented and composite  $AL_{ILM}$  measurements increased as AL increased (Fig. 1). The segmented  $AL_{ILM}$  was up to 0.32 mm shorter in an eye with a composite  $AL_{ILM}$  of 33.01 mm which is the longest eye in this study.

The mean absolute refractive error (MAE) was  $0.42 \pm 0.38$  D using the composite  $AL_{ILM}$ , and  $0.41 \pm 0.36$  D using the segmented  $AL_{ILM}$ . There was no significant difference in the MAE ( $P = 0.35$ ).

A subgroup analysis was performed for the 15 extra-long eyes implanted with low power IOLs ( $\leq +4.00$  D). The same model of IOL (AN6MA) were implanted in these 15 eyes. The mean composite  $AL_{ILM}$  was  $31.02 \pm 0.85$  mm (range: 29.80 to 33.01 mm) and the mean segmented  $AL_{ILM}$  was  $30.78 \pm 0.82$  mm (range: 29.61 to 32.69 mm, Table 2), which was significantly different ( $P < 0.001$ ). The mean difference between composite and segmented  $AL_{ILM}$  measurements in extra-long eyes was  $0.24 \pm 0.03$  mm.

The MAE using the segmented  $AL_{ILM}$  was  $0.45 \pm 0.86$  D, which was significantly smaller than the MAE using the composite  $AL_{ILM}$  ( $0.80 \pm 0.86$  D,  $P < 0.001$ ). Additionally, the percentage of correct refraction predictions within  $\pm 0.25$  D,  $\pm 0.50$  D, and  $\pm 1.00$  D were 53.3%, 66.7%, and 86.7%, respectively, with segmented  $AL_{ILM}$  measurements and 33.3%, 53.3%, and 73.3%, respectively, with composite  $AL_{ILM}$  measurements (Table 2). There were significant differences in the percentage of refractive prediction errors between segmented and composite measurements within  $\pm 0.50$  D ( $P = 0.003$ ) and  $\pm 1.00$  D ( $P = 0.01$ ), but not  $\pm 0.25$  D ( $P = 0.18$ ).

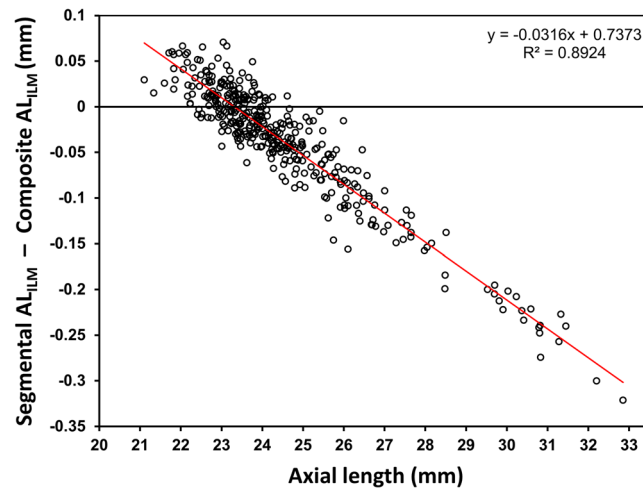


**Figure 1.** Bland–Altman plots showing the agreement between segmented and composite  $AL_{ILM}$  measurements. The solid line indicates the best-fit line ( $R^2 = 0.89$ ,  $P < 0.001$ ). AL = axial length, ILM = inner limiting membrane.

	Composite Method	Segmental method	P
Mean $AL_{ILM}$ (mm)	$31.02 \pm 0.85$	$30.78 \pm 0.82$	$< 0.001$
Minimum axial length (mm)	29.80	29.61	—
Maximum axial length (mm)	33.01	32.69	—
Mean spherical equivalent (D)	$0.80 \pm 0.86$	$0.45 \pm 0.86$	$< 0.001$
Mean absolute error (D)	$0.80 \pm 0.86$	$0.57 \pm 0.78$	$< 0.001$
Median absolute error (D)	0.46	0.23	—
Median absolute error 95% CI	0.32–1.27	0.14–1.00	—
Number and percentage of eyes within prediction error			
$\pm 0.25$ D	5 (33.3%)	8 (53.3%)	0.18
$\pm 0.50$ D	8 (53.3%)	10 (66.7%)	0.003
$\pm 1.00$ D	11 (73.3%)	13 (86.7%)	0.01

**Table 2.** Predicted refractive outcomes using the composite and segmental methods in extremely long (axial length  $> 29$  mm) eyes implanted less than 4.0 diopter intraocular lens ( $n = 15$  eyes). Data are presented as the mean standard deviation. The Haigis formula was used to calculate intraocular lens power. AL = axial length, CI = confidence interval, D = diopters, ILM = inner limiting membrane.

## Discussion

The AL can be calculated in a variety of ways, as shown in Fig. 2. These differences arose from changes in technology and measurement compatibility with IOL power calculation formulas. Since the segmental method with the ultrasound immersion technique is more accurate than the composite method with the ultrasound contact technique, we speculated that the optical measurements with the segmental method would be more precise than the conventional ones with the composite method. Therefore, the present study compared the composite and segmental methods of obtaining optical  $AL_{ILM}$  measurements. We found that the difference between the segmental and composite methods in optical  $AL_{ILM}$  measurements had a negative proportional bias with AL. This is because the regression Eq. (1) was used to adjust the composite  $AL_{RPE}$  to the composite  $AL_{ILM}$ . As the  $AL_{RPE}$  coefficient is 1.0446 (calculated by dividing 1.0 by 0.9573),  $AL_{ILM}$  was overestimated in the longer eye using Eq. (1). On the other hand, regarding vitreous length, which is often longer in the longer eye (see Supplementary Fig. S1), the calculated segmented AL is longer than the composite AL due to the difference between the reflective index of the vitreous (1.336), and the mean refractive index of the whole eye (1.349). However, this difference is smaller than the effect of the regression Eq. (1). Therefore, the  $AL_{ILM}$  was significantly shorter when acquired with the segmental method than with the composite method in highly myopic eyes. The IOL power calculation using the Haigis formula with segmented  $AL_{ILM}$  resulted in a smaller post-operative hyperopic shift than that using the composite  $AL_{ILM}$  in the subgroup analysis.

Many IOL power calculation formulas were developed before PCI-based optical biometers were invented. Therefore, one needs to rely upon the ultrasound  $AL_{ILM}$ <sup>4</sup>. The ultrasound  $AL_{ILM}$  with the immersion technique is shorter than the optical  $AL_{RPE}$  with the composite method; this difference could induce post-operative refraction errors<sup>7</sup>. Therefore, an established conversion algorithm between optical  $AL_{RPE}$  measurements with the composite

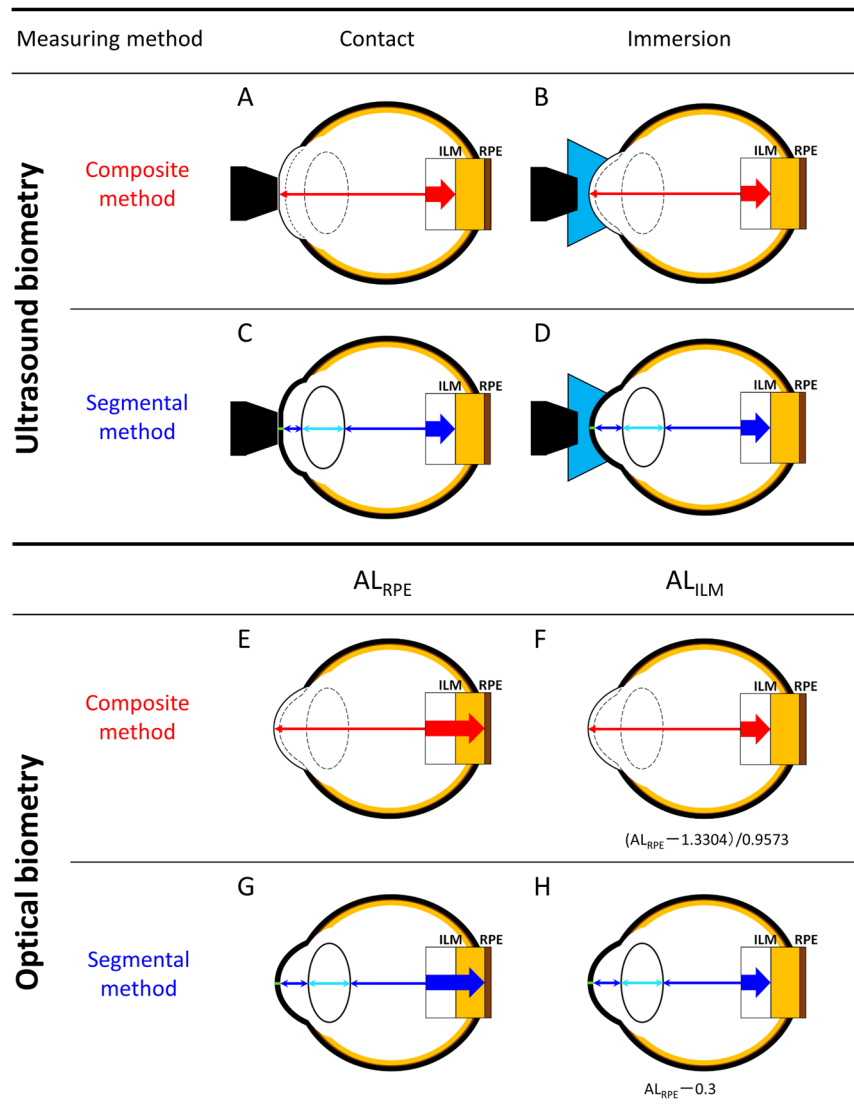


**Figure 2.** An overview of axial length (AL) measurement strategies for ultrasound and optical AL measurements. (A–D) Acoustic contact and immersion measurements made using mean group (composite; A,B) and individual tissue (segmental; C,D) sound velocity. Optical AL measurements using the composite (E,F) and segmental (G,H) methods. Optical systems (E,G) measure the linear distance between the corneal surface and the retinal pigment epithelium (RPE,  $AL_{RPE}$ ) and optical systems (F,H) measure the linear distance between the corneal surface and the inner limiting membrane (ILM,  $AL_{ILM}$ ). Since intraocular lens power calculation formulas were developed using the  $AL_{ILM}$ , each segmented  $AL_{RPE}$  measurement was converted to an  $AL_{ILM}$  by subtracting the retinal thickness (assumed to be 300  $\mu\text{m}$  in all eyes). Optical composite  $AL_{RPE}$  measurements were converted to  $AL_{ILM}$  measurements using a regression equation:  $AL_{ILM} = (AL_{RPE} - 1.3304) / 0.9573$ .

method and immersion ultrasound  $AL_{ILM}$  measurements with the segmental method has been used for a long time<sup>7</sup>. This algorithm, however, is subject to limitations such as an inadequate retinal thickness measurement in eyes with longer ALs. For example, an eye with a 30.0 mm  $AL_{ILM}$  should have a retinal thickness of 49  $\mu\text{m}$  (achieved composite  $AL_{RPE}$  minus composite  $AL_{ILM}$ ), but an eye with a 20.0 mm  $AL_{ILM}$  should have a retinal thickness of 476  $\mu\text{m}$  (10-fold difference). This may be one of the reasons why ALs in long and short eyes tend to be less accurate for predicting refractive outcomes following cataract surgery. In previous studies, the segmented ALs measured by an optical biometer with an 820 nm wavelength were longer in short eyes and shorter in long eyes compared to the composite ALs<sup>8,9</sup>. In the current study, the relationship between segmented and composite  $AL_{ILM}$  obtained by SS-OCT with a wavelength of 1060 nm was similar to that reported previously<sup>8,9</sup>.

Although the most significant source of error that contributes to post-operative refractive error comes from the AL<sup>17</sup>, errors in predicted post-operative IOL positions have also become a major contributor to post-operative refractive errors after the introduction of laser biometry<sup>1,2,18</sup>. The post-operative IOL position no longer influences post-operative refractive errors when low power IOLs (<+4.0 D) are used; even a 1.0 mm forward movement in

Intraocular lens power	Refractive outcome 3-mm position (D)	Refractive outcome 4-mm position (D)	Refractive outcome change (D)
3.0 D	0.00	0.10	-0.10
4.0 D	-0.80	-0.60	-0.20
5.0 D	-1.60	-1.30	-0.30
7.0 D	-3.20	-2.80	-0.40
8.0 D	-4.10	-3.60	-0.50

**Table 3.** Theoretical change in refractive outcome with a 1-mm anterior shift in intraocular lens position. Refractive outcomes are presented as the spherical equivalent. Theoretical refractive outcomes were calculated using optical design software with the ray-tracing method. All calculations were made assuming an axial length of 30 mm, an anterior corneal curvature radius of 7.8 mm, and a posterior corneal curvature radius of 6.5 mm. D = diopters.

a low power IOL position (e.g., from 4.0 mm to 3.0 mm) influences the refractive outcome by less than  $-0.2$  D, as demonstrated in Table 3. However, the high power IOL has a big influence on the refractive outcome. Therefore, we performed a subgroup analysis on patients that received an IOL with a power less than  $+4.0$  D.

Previous studies have documented inaccuracies of the popular IOL formulas in long eyes<sup>19–25</sup>. Although the Haigis formula generally has better refractive outcomes in long eyes, post-operative hyperopic errors proportional to the AL have been reported<sup>23</sup>.

The current study did not find a significant difference between predicted post-operative refractive errors when the segmental method and composite method measurements of optical AL were examined in all eyes. However, the post-operative hyperopic shift with the Haigis formula was significantly improved in highly myopic eyes when the optical  $AL_{ILM}$  acquired with the segmental method was used. Although the simple replacement of the composite  $AL_{ILM}$  with the segmented  $AL_{ILM}$  in the traditional IOL power calculations would not help because many formulas are optimised for the composite  $AL_{ILM}$ , recent studies reported that the segmented AL measured via an optical biometer with a peak wavelength of 820 nm improved refractive prediction accuracy for vergence formulas<sup>8,9</sup>.

Our study had several limitations. First, it is a retrospective single centre study and the population in our subgroup study was relatively small. We used two different IOLs; further investigation of segmented AL measurements in a prospective multicentre study with a larger group of patients and with one model is desirable. Second, the fixation status during the measurement is an important factor for AL accuracy. The SS-OCT biometer enables us to obtain an optical B-scan image during AL measurement. Therefore, it is now possible to check the fixation status during AL measurements and to examine complete longitudinal cross-sectional images of the eye<sup>26–29</sup>. Further studies that utilise these SS-OCT capabilities are needed. Third, our study only measured the effect of AL characteristics on post-operative refractive outcomes. However, other factors are known to influence the refractive outcomes in cataract surgery. The corneal power, in particular, should be investigated more carefully because prior studies have shown that standard keratometry overestimates the corneal power<sup>24</sup>. Finally, the mean group refractive index can vary with cataract grade<sup>30</sup>, and adjustments may be needed for cataract types and stages in future studies.

In conclusion, the segmented  $AL_{ILM}$  is more accurate than the conventional one measured with the composite method when using SS-OCT, and the segmented AL measurement reduces the post-operative hyperopic shift in eyes with extra-long AL.

## Methods

**Study participants.** This was a retrospective, consecutive case series of all patients who had undergone uncomplicated cataract surgery at a single centre, the National Hospital Organization, Tokyo Medical Center between October 2015 and January 2018. The protocol was reviewed and approved by the Institutional Review Board of the National Hospital Organization, Tokyo Medical Center, and was designed in accordance with the tenets of the Declaration of Helsinki. Informed consent was obtained from all patients. The selection criteria of this study followed the recommendations of a recent editorial by Hoffer *et al.*<sup>31</sup> regarding best practices for studies of IOL formulas: the use of optical biometry and the inclusion of only 1 eye from each study subject. If patients underwent bilateral cataract surgery, then a randomly selected eye was chosen for inclusion in the study. The exclusion criteria were a best-corrected distance visual acuity after cataract surgery worse than 20/40, a history of ocular surgery, a history of ocular trauma, the presence of a significant ocular comorbidity, unreliable or undetectable preoperative biometry measurements, or a history of intra- or post-operative complications.

All patients underwent cataract surgery through a 2.2-mm corneal incision. One of the following IOLs was implanted: AcrySof Toric (SN6A T3-T6, Alcon, Fort Worth, TX) or AN6MA (KOWA, Nagoya, Japan). All surgical procedures were performed under topical anaesthesia by the same experienced surgeon (TN) and all IOLs were successfully inserted into the capsular bag after phacoemulsification.

**Data collection and patient examinations.** All data were retrospectively collected from patient medical records. All patients had undergone preoperative and 1-month post-operative ophthalmic examinations, including a slit-lamp examination, keratometry, and funduscopy. SS-OCT based biometer (OA-2000; TOMEY CORPORATION, Nagoya, Japan) and AS-OCT (CASIA2; TOMEY CORPORATION) were performed

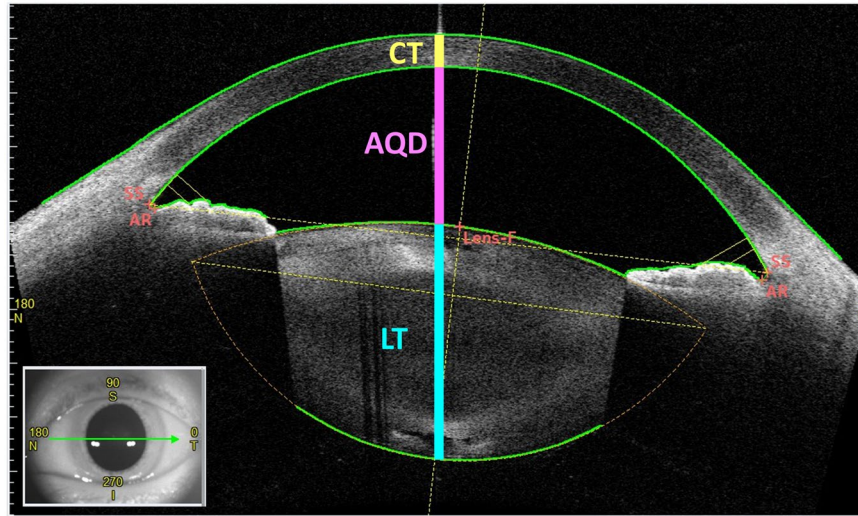


**Figure 3.** An anterior segment optical coherence tomography (OCT) image showing optical biometer measurements. Measurements were made before cataract surgery along the vertex normal. The inset shows an external photograph with the location and direction of the OCT scan (green arrow). CT = corneal thickness, AQD = aqueous depth, LT = crystalline lens thickness, Lens-f = lens fornix, AR = angle recess, SS = scleral spur, N = nasal, S = superior, T = temporal, I = inferior.

preoperatively. Distant corrected visual acuity, refraction, and intraocular pressure were also measured only by experienced technicians.

*Swept-source optical coherence tomography based biometer.* The SS-OCT based biometer was used to measure AL and corneal power, along with corneal thickness, ACD, and lens thickness using the swept-source laser (1060 nm wavelength). The biometer obtained 10 consecutive scans and automatically calculated the average value.

*Anterior segment optical coherence tomography.* The angle analysis mode in CASIA2 was used to obtain anterior segment images comprising 16 consecutive meridional scans. This instrument uses a super-luminescent diode light source (1310 nm wavelength) and has a scan speed of 50,000 A-scans/second. All OCT images were obtained while the pupil was dilated (topical 0.5% tropicamide and 0.5% phenylephrine hydrochloride). All eyes were imaged in a dark room (illuminance of 0.3 lx) using internal fixation and were obtained twice by a trained technician who was masked to the clinical data.

Only images taken with a horizontal (180°) alignment were used in the analysis. Images were centred on the corneal vertex, which was defined as the cross point of the vertex normal and anterior corneal surface. The AS-OCT parameters measured along the vertex normal included corneal thickness, ACD, AQD, and lens thickness. Corneal thickness was defined as the distance between the anterior and posterior corneal surfaces, ACD is the distance between the anterior corneal and anterior lens surfaces, AQD is the distance between the posterior corneal and anterior lens surfaces, and lens thickness is the distance between the anterior and posterior lens surfaces (Fig. 3). The corneal thickness, AQD, and lens thickness were measured by two independent examiners (SG, II) who were masked to the clinical data.

*Definition of axial length.* Figure 2 illustrates how AL was obtained using acoustic and optical measurements. To measure AL, systems used either the composite method, which utilises the mean group index, or the segmental method, which accounts for individual tissue indices of the cornea, aqueous, lens, and vitreous. Ultrasound biometry can measure AL in the following four ways: acoustic contact measurements using mean group sound velocity (Fig. 2A), acoustic immersion measurements using mean group sound velocity (Fig. 2B), acoustic segmented contact measurements using individual sound velocities (Fig. 2C), and acoustic segmented immersion measurements using individual sound velocities (Fig. 2D). Segmented immersion is theoretically the most accurate acoustic measurement because the ultrasound probe does not directly contact the cornea (Fig. 2D).

On the other hand, the SS-OCT based optical biometer measures the optical path length of the whole eye. Currently, it is essential for the optical AL measurement to determine  $AL_{ILM}$  from the  $AL_{RPE}$ , as popular IOL power formulas do not use  $AL_{RPE}$  but use  $AL_{ILM}$  measurements instead. To estimate composite distance measurements between the cornea and RPE ( $AL_{RPE}$ , Fig. 2E), the SS-OCT based biometer system uses a mean group refractive index of 1.3496. Then, the following equation (Eq. 1), which is publicly available through the manufacturer, was used to translate  $AL_{RPE}$  into composite distance measurements between the cornea and ILM ( $AL_{ILM}$ , Fig. 2F) in the current study:

$$\text{Composite AL}_{\text{ILM}} = (\text{Composite AL}_{\text{RPE}} - 1.3304)/0.9573 \quad (1)$$

The segmented  $\text{AL}_{\text{RPE}}$  is measured as the sum of the thickness of the cornea, aqueous, lens, and vitreous (Fig. 2G). The refractive indices of the cornea, aqueous, lens, and vitreous were set to 1.376, 1.336, 1.410, and 1.336, respectively<sup>26,32</sup>. Refractive indices of the individual tissue were used during the calculation. The corneal thickness, AQD, and lens thickness were directly measured using AS-OCT. The optical vitreous length was calculated by subtracting the optical path length of the corneal thickness, AQD, and the lens thickness obtained by AS-OCT from the optical path length of the whole eye obtained using an SS-OCT based biometer. Finally, the optical vitreous length was divided by the refractive index of vitreous (1.336) to obtain the vitreous length. The segmented  $\text{AL}_{\text{ILM}}$  (Fig. 2H) was then calculated by subtracting the retinal thickness (previously established as  $300\ \mu\text{m}$ <sup>33–35</sup>) from the segmented  $\text{AL}_{\text{RPE}}$ .

**Formula calculations.** The Haigis formula<sup>7</sup> was calculated using Excel spreadsheets (Microsoft Corporation, Redmond, WA, USA), and was checked against licensed commercial software on the SS-OCT based biometer. The optimised lens constants from the User Group for Laser Interference Biometry (ULIB) were used for calculations (AcrySof Toric:  $a_0 = 1.78$ ,  $a_1 = 0.40$ , and  $a_2 = 0.10$  and AN6MA:  $a_0 = 1.57$ ,  $a_1 = 0.40$ , and  $a_2 = 0.10$ )<sup>36</sup>.

**Data analysis.** Composite and segmented  $\text{AL}_{\text{ILM}}$  measurements were compared by using the paired t-test. Bland–Altman plots were used to assess the agreement between the composite and segmented  $\text{AL}_{\text{ILM}}$ . The mean post-operative refractive errors (post-operative spherical equivalent minus the predicted post-operative spherical equivalent), mean absolute prediction error (MAE), median absolute prediction error, and standard deviation of the prediction error were calculated with the composite  $\text{AL}_{\text{ILM}}$  and the segmented  $\text{AL}_{\text{ILM}}$ . The Wilcoxon test was used to compare the MAE values. Subgroup analysis was performed on eyes in which low power IOL less than  $+4.0\ \text{D}$  were implanted. The percentages of eyes with arithmetic prediction errors within  $\pm 0.25\ \text{D}$ ,  $\pm 0.50\ \text{D}$ , and  $\pm 1.0\ \text{D}$  were compared between the composite  $\text{AL}_{\text{ILM}}$  and the segmented  $\text{AL}_{\text{ILM}}$  using the McNemar test. Statistical significance was defined as  $P < 0.05$ . All statistical analyses were performed using JMP Pro statistical software (version 10.0.2, SAS Institute Inc., Cary, NC, USA).

### Data availability

The datasets generated during and/or analysed during the current study are available from the corresponding author on reasonable request.

Received: 25 November 2019; Accepted: 4 February 2020;

Published online: 11 March 2020

### References

- Norrby, S. Sources of error in intraocular lens power calculation. *J. Cataract. Refract. Surg.* **34**, 368–376 (2008).
- Olsen, T. Calculation of intraocular lens power: a review The statistical. *Acta Ophthalmol Scand* 2007:472–485.
- Hoffer, K. J. Ultrasound velocities for axial eye length measurement. *J. Cataract. Refract. Surg.* **20**, 554–562 (1994).
- Drexler, W. *et al.* Partial coherence interferometry: a novel approach to biometry in cataract surgery. *Am. J. Ophthalmol.* **126**, 524–534 (1998).
- Roy, A., Das, S., Sahu, S. K. & Rath, S. Ultrasound Biometry vs. IOL Master. *Ophthalmol.* **119**, 29–31 (2012).
- Rajan, M. S., Keilhorn, I. & Bell, J. A. Partial coherence laser interferometry vs conventional ultrasound biometry in intraocular lens power calculations. *Eye* **16**, 552–556 (2002).
- Haigis, W., Lege, B., Miller, N. & Schneider, B. Comparison of immersion ultrasound biometry and partial coherence interferometry for intraocular lens calculation according to Haigis. *Graefes Arch. Clin. Exp. Ophthalmol.* **238**, 765–773 (2000).
- Cooke, D. L. & Cooke, T. L. A comparison of two methods to calculate axial length. *J. Cataract. Refract. Surg.* **45**, 284–292 (2019).
- Wang, L., Cao, D., Weikert, M. P. & Koch, D. D. Calculation of axial length using a single group refractive index versus using different refractive indices for each ocular segment: theoretical study and refractive outcomes. *Ophthalmol.* **126**, 663–670 (2018).
- Chansangpetch, S. *et al.* Agreement of Anterior Segment Parameters Obtained From Swept-Source Fourier-Domain and Time-Domain Anterior Segment Optical Coherence Tomography. *Invest. Ophthalmol. Vis. Sci.* **59**, 1554–1561 (2018).
- Kimura, S. *et al.* Assessment of tilt and decentration of crystalline lens and intraocular lens relative to the corneal topographic axis using anterior segment optical coherence tomography. *PLoS One* **12**, 1–12 (2017).
- Shoji, T. *et al.* *In vivo* crystalline lens measurements with novel swept-source optical coherent tomography: an investigation on variability of measurement. *BMJ Open. Ophthalmol.* **1**, e000058 (2017).
- Reitblat, O., Levy, A., Kleinmann, G. & Assia, E. I. Accuracy of intraocular lens power calculation using three optical biometry measurement devices: the OA-2000, Lenstar-LS900 and IOLMaster-500. *Eye* **32**, 1244–1252 (2018).
- McAlinden, C. *et al.* Axial length measurement failure rates with biometers using swept-source optical coherence tomography compared to partial-coherence interferometry and optical low-coherence interferometry. *Am. J. Ophthalmol.* **173**, 64–69 (2017).
- Savini, G. *et al.* Accuracy of a new swept-source optical coherence tomography biometer for IOL power calculation and comparison to IOLMaster. *J. Refract. Surg.* **33**, 690–695 (2017).
- Gao, R. *et al.* Comparison of ocular biometric measurements between a new swept-source optical coherence tomography and a common optical low coherence reflectometry. *Sci. Rep.* **7**, 2484 (2017).
- Olsen, T. Sources of error in intraocular lens power calculation. *J. Cataract. Refract. Surg.* **18**, 125–129 (1992).
- Goto, S. *et al.* Prediction of postoperative intraocular lens position with angle-to-angle depth using anterior segment optical coherence tomography. *Ophthalmol.* **123**, 2474–2480 (2016).
- Melles, R. B., Holladay, J. T. & Chang, W. J. Accuracy of Intraocular Lens Calculation Formulas. *Ophthalmol.* **125**, 288–294 (2018).
- Bang, S. *et al.* Accuracy of intraocular lens calculations using the IOLMaster in eyes with long axial length and a comparison of various formulas. *Ophthalmol.* **118**, 503–506 (2011).
- Wang, J. K., Hu, C. Y. & Chang, S. W. Intraocular lens power calculation using the IOLMaster and various formulas in eyes with long axial length. *J. Cataract. Refract. Surg.* **34**, 262–267 (2008).
- Abulafia, A. *et al.* Intraocular lens power calculation for eyes with an axial length greater than 26.0 mm: Comparison of formulas and methods. *J. Cataract. Refract. Surg.* **41**, 548–556 (2015).
- Wang, Q. *et al.* Accuracy of intraocular lens power calculation formulas in long eyes: A systematic review and meta-analysis. *Clin Exp Ophthalmol* (2018).

24. Olsen, T. Intraocular lens power calculation errors in long eyes. *J. Cataract. Refract. Surg.* **38**, 733–734 (2012).
25. Yokoi, T. *et al.* Evaluation of refractive error after cataract surgery in highly myopic eyes. *Int. Ophthalmol.* **33**, 343–348 (2013).
26. Shamma, H. J. *et al.* Biometry measurements using a new large-coherence-length swept-source optical coherence tomographer. *J. Cataract. Refract. Surg.* **42**, 50–61 (2016).
27. Whang, W. J., Yoo, Y. S., Kang, M. J. & Joo, C. K. Predictive accuracy of partial coherence interferometry and swept-source optical coherence tomography for intraocular lens power calculation. *Sci. Rep.* **8**, 1–10 (2018).
28. Omoto, M. K. *et al.* Ocular biometry and refractive outcomes using two swept-source optical coherence tomography-based biometers with segmental or equivalent refractive indices. *Sci. Rep.* **9**, 6557 (2019).
29. Akman, A., Asena, L. & Güngör, S. G. Evaluation and comparison of the new swept source OCT-based IOLMaster 700 with the IOLMaster 500. *Br. J. Ophthalmol.* **100**, 1201–1205 (2016).
30. Prinz, A. *et al.* Influence of severity of nuclear cataract on optical biometry. *J. Cataract. Refract. Surg.* **32**, 1161–1165 (2006).
31. Hoffer, K. J. *et al.* Protocols for studies of intraocular lens formula accuracy. *Am. J. Ophthalmol.* **160**, 403–405.e1 (2015).
32. Goncharov, A. V. & Dainty, C. Wide-field schematic eye models with gradient-index lens. *J. Opt. Soc. Am. A Opt Image Sci. Vis.* **24**, 2157–2174 (2007).
33. Myers, C. E. *et al.* Retinal thickness measured by spectral-domain optical coherence tomography in eyes without retinal abnormalities: the Beaver Dam Eye Study. *Am. J. Ophthalmol.* **159**, 445–456 (2015).
34. Duan, X. R. *et al.* Normal macular thickness measurements using optical coherence tomography in healthy eyes of adult Chinese persons: The Handan Eye Study. *Ophthalmol.* **117**, 1585–1594 (2010).
35. Chan, A. *et al.* Normal macular thickness measurements in healthy eyes using Stratus optical coherence tomography. *Arch. Ophthalmol.* **124**, 193–8 (2006).
36. User Group for Laser Interference Biometry (ULIB). Available at, <http://ocusoft.de/ulib>; (Oct 31, 2016. Accessed May 10, 2018).

## Acknowledgements

The authors thank Keiko Ogawa, CO, Saori Sugiyama, CO, and Maki Matsumaru, CO, (Orthoptists of National Hospital Organization, Tokyo Medical Center) for their assistance with data collection.

## Author contributions

S.G., N.M., T.N. K.O., I.I., S.K. and K.N. designed the concept of this study. S.G., T.N. and I.I. collected the data. S.G., N.M. and T.N. conducted statistical analysis. S.G., N.M., T.N. and I.I. interpreted the data. S.G., N.M. and T.N. drafted the work. S.G., N.M., T.N. K.O., I.I., S.K. and K.N. revised it critically for important intellectual content. S.G., N.M., T.N. K.O., I.I., S.K. and K.N. approved of the version submitted for publication. All author agreed to be accountable for all aspects of the work in ensuring that questions related to the accuracy or integrity of any part of the work are appropriately investigated and resolved.

## Competing interests

Drs. Goto, Maeda, Noda, and Nishida received fees from TOMEY CORPORATION for a sponsored seminar not related to this study. No conflicting relationship exists for any other author.

## Additional information

**Supplementary information** is available for this paper at <https://doi.org/10.1038/s41598-020-61391-7>.

**Correspondence** and requests for materials should be addressed to N.M.

**Reprints and permissions information** is available at [www.nature.com/reprints](http://www.nature.com/reprints).

**Publisher's note** Springer Nature remains neutral with regard to jurisdictional claims in published maps and institutional affiliations.



**Open Access** This article is licensed under a Creative Commons Attribution 4.0 International License, which permits use, sharing, adaptation, distribution and reproduction in any medium or format, as long as you give appropriate credit to the original author(s) and the source, provide a link to the Creative Commons license, and indicate if changes were made. The images or other third party material in this article are included in the article's Creative Commons license, unless indicated otherwise in a credit line to the material. If material is not included in the article's Creative Commons license and your intended use is not permitted by statutory regulation or exceeds the permitted use, you will need to obtain permission directly from the copyright holder. To view a copy of this license, visit <http://creativecommons.org/licenses/by/4.0/>.

© The Author(s) 2020